Advanced and Sustainable Technologies
ASET
E-ISSN 2976-2294
Volume 3, No 2, December 2024 [30-41]

Computational Fluid Dynamics Analysis of Under-door Exhaust Duct: Influences of Inlet Diameter and Number of Outlet Holes

Jun Yuan Phong[1*]

[1]Faculty of Mechanical Engineering & Technology, Universiti Malaysia Perlis (UniMAP), 02600 Arau, Perlis, Malaysia

Received 5 August 2024, Revised 30 August 2024, Accepted 1 September 2024

ABSTRACT

This paper analyses the duct flow pressure and velocity using SimFlow 4.0, a Computational Fluid Dynamics (CFD) software. The primary objective of the study is to investigate the fluid behavior within duct systems, focusing on critical parameters such as pressure distribution and velocity profiles. The simulation considers two independent parameters: the inlet diameter of the duct flow and the number of the outlet duct flow. The results demonstrate that the variations in duct design and inlet conditions influence the overall performance, highlighting critical regions of pressure distribution and velocity changes. The correlations between the inlet diameter and number of outlets with the pressure and velocity are studied. This analysis provides valuable insights for optimizing ductwork in various engineering applications, ensuring efficient and effective fluid transport. Besides, the study emphasizes the importance of CFD tools like SimFlow in predicting and enhancing the performance of duct systems.

Keywords: Computational fluid dynamics, SimFlow, Under-door Exhaust Duct, Simulation and modeling.

1. INTRODUCTION

Computational Fluid Dynamics (CFD) is a crucial tool in analyzing and optimizing duct flow in various engineering applications, ranging from aerospace to power generation. The primary objective of using CFD in duct flow analysis is to predict and enhance the performance characteristics of different duct configurations. This method employs numerical analysis and algorithms to solve and analyze fluid flows, providing detailed insights into the behavior of gases and liquids within ducts. The advancements in CFD techniques have enabled engineers to design more efficient duct systems by optimizing parameters such as velocity distribution, pressure drop, and heat transfer, leading to significant performance and energy efficiency improvements.

Several studies have demonstrated the efficacy of CFD in duct flow analysis. For instance, Brankovic et al. [1] utilized CFD to analyze the flow in the turnaround duct of the Space Shuttle Main Engine, highlighting the importance of duct configuration and diffuser strut alignment in enhancing flow understanding and duct performance [1]. Similarly, Anand et al. (2010) [2] conducted a computational investigation on a Y-shaped diffusing duct, revealing the impact of secondary flows induced by curvature and changes in cross-sectional area on performance characteristics (Anand, 2010). Experimental and CFD studies by Gu et al. (2009) [3] on fluid dynamic gauging in duct flows confirmed the validity of CFD simulations in predicting stresses and gauging practical working ranges, demonstrating close agreement with experimental data (Gu, 2009). Further, Avvari et al. (2016) [4] developed a flow control algorithm using CFD to

*Corresponding author: phongjunyuan02@gmail.com

optimize guide vane placement in power plant ducts, illustrating the tool's utility in industrial applications (Avvari, 2016). CFD analysis has been used in power plant applications to ensure the even distribution of hot gases within ducts. Devakumaran et al. (2018) [5] analyzed gas duct configurations using CFD to achieve uniform flow distribution by modifying duct designs and incorporating guide plates. Boonloi et al. (2022) [6] examined the effects of baffle height and location on heat transfer and flow profiles in a baffled duct, showing significant enhancements in heat transfer efficiency with optimal baffle placement. These studies collectively underscore the versatility and effectiveness of CFD in optimizing duct flow across various applications, contributing to advancements in design and operational efficiency.

Moreover, Lopez et al. [7] examined the penetration of underfloor air distribution (UFAD) systems in the residential and commercial air conditioning industries, noting their prominent use in data centers due to demanding thermal requirements. It highlights the advantages of UFAD over traditional overhead (OH) systems. It compares four different UFAD ventilation layouts with one OH layout. Their findings indicated that multiple swirl-type diffusers in UFAD systems provide a more uniform floor-to-knee temperature and reduce air recirculation compared to rectangular grille-type diffusers. Positioning return vents on the room's sides created a cooler environment by confining recirculating air to a smaller area. He et al. [8] studied the ventilation performance can affect thermal comfort and building energy by investigating the efficiency of China's first certified Active House building. They highlighted that roof windows enhanced ventilation efficiency by up to 1.62 times compared to mechanical systems and emphasized the importance of the roof window and door opening design in generating effective airflow. They found that factors such as indoor space geometry, local climate, and ground-source heat pumps all synthetically influence ventilation performance, underscoring the need for a holistic design strategy for sustainable building design. Fan et al. [9] focused on using underfloor air distribution (UFAD) systems, recognized for their benefits in energy efficiency, indoor air quality, and thermal comfort. Utilizing a computational fluid dynamics (CFD) simulation with ANSYS Fluent, the research investigates a large circular underfloor plenum in a conference room equipped with 503 under-seat diffusers, examining the impact of internal air velocity and static pressure distributions on airflow uniformity to the occupied zones. They compared one concentrated air supply mode with three uniform air supply modes, concluding that the configuration of multiple supply ducts with bottom air outlets provides the best uniformity of supply air. Chao et al. [10] addressed the high risk of nosocomial infection among healthcare workers (HCWs) due to their exposure to bioaerosols during procedures on infectious patients, such as endotracheal intubations for severe acute respiratory syndrome (SARS). Local exhaust ventilation (LEV) has been proposed to lower bioaerosol concentration in hospital wards to mitigate this risk. Computational fluid dynamic (CFD) models were developed to simulate the transport of infectious droplets and bioaerosols, focusing on the design and control of LEV systems. They detailed these CFD models and analyzed droplet and bioaerosol distribution and suspension based on size, emission direction, and speed, demonstrating that a well-designed LEV system effectively removes infectious particles from the HCW's breathing zone.

The current study aims to investigate the effects of ducting inlet diameter and outlet count on the internal flow characteristics using SimFlow software with the steady-state method. By analyzing different duct diameters, we seek to understand the independent parameters influencing dependent parameters, such as velocity distribution, pressure drop, and turbulence within the ducts. The steady-state method will allow us to obtain a detailed and accurate picture of the flow behavior under constant conditions. The insights gained from this study are expected to benefit society by improving our understanding of airflow in enclosed spaces, leading to more efficient Heating, Ventilation, and Air Conditioning (HVAC) system designs and better indoor air quality. Enhanced knowledge of duct flow also contributes to energy savings and environmental sustainability by optimizing airflow distribution and reducing energy consumption in buildings.

2. MATERIAL AND METHODS

The geometry of the simplified Under-door Exhaust Duct, as shown in Figure 1, was exactly prepared for meshing and simulation using the SimFlow software [11]. The study was designed to estimate the maximum velocity and pressure within the duct under varying conditions. The diameter of the inlet was adjusted across three values: 240 mm, 260 mm, and 280 mm, while the number of holes at the outlet varied between 2, 4, and 6. Each configuration was assessed at a velocity of 0.5 m/s. The different designs of the under-door exhaust duct are shown in Figure 2. The computational fluid dynamics model employed the Reynolds-Averaged Navier-Stokes (RANS) k-ω turbulence model [12] to capture the flow characteristics. Mesh refinement in SimFlow enhanced the element quality around the under-door exhaust duct, ensuring accurate simulation results.

The autofill feature defined the base mesh parameters, automatically creating the flow domain to facilitate the simulation via the material points setting. A mesh division of (25, 25, 25) was set, resulting in a hexahedral-dominant mesh configuration for both the domain and the model. This mesh division led to the generation of 10,692 mesh elements (Figure 3 b). To simulate the physical scenario accurately, boundary conditions were defined on the domain surfaces. These included the specification of inlet velocity, pressure at the outlet, and the properties of the walls (Figure 3 a). The simulation was conducted under the assumption of steady-state, incompressible flow conditions, using the SIMPLE (Semi-Implicit Method for Pressure-Linked Equations) [13] discretization solver. The slice feature was employed for results visualization, allowing a detailed examination of flow characteristics within the duct. This setup was repeated eight additional times, each with different inlet diameters and numbers of outlet holes, to thoroughly explore the impact of these variables on the flow characteristics within the duct system.

The meshing process for the different models involved generating grids with varying inlet diameters and the number of outlet holes, as summarized in Table 1. This detailed meshing was crucial for accurately capturing the flow dynamics within the under-door exhaust duct across different configurations. The meshing process for different inlet diameters and outlet hole configurations in the under-door exhaust duct was designed to capture accurate flow dynamics while balancing computational efficiency. As the inlet diameter increased from 240 mm to 280 mm, the mesh quality improved, indicated by higher node and cell counts and reduced skewness and aspect ratios. This progression resulted in more refined and uniform meshes, essential for precise flow simulations. Each configuration's mesh adjustments ensured that the simulations accurately represented the flow characteristics within the duct, optimizing both accuracy and computational resources.

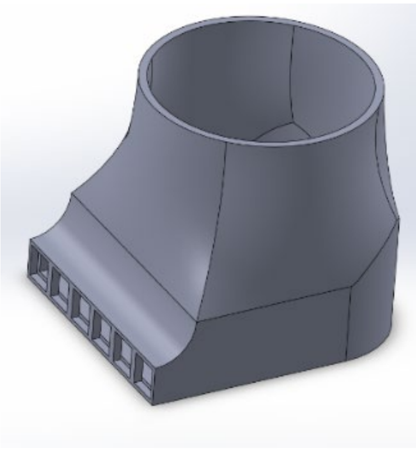

Figure 1: 3D model of under-door exhaust duct.

Inlet Diameter	Number of outlet holes		
	2	4	6
240 mm	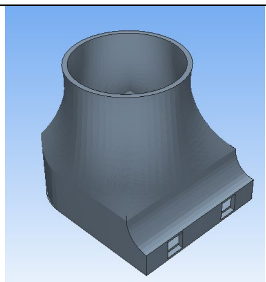	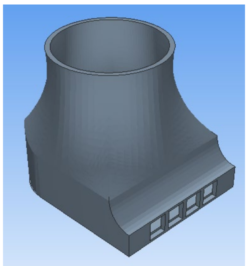	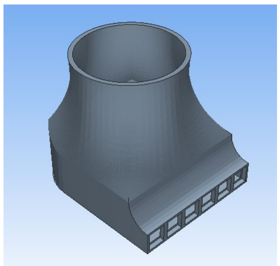
260 mm	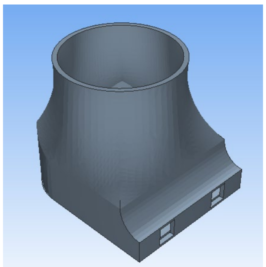	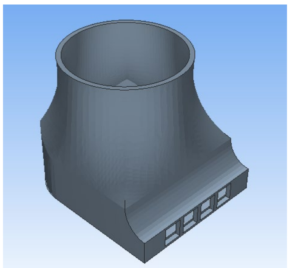	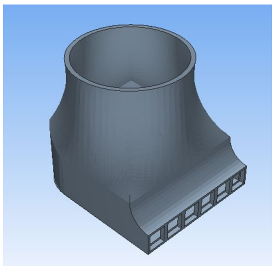
280 mm	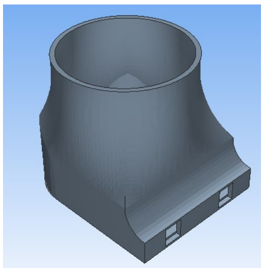	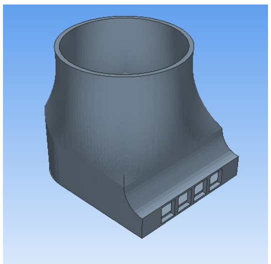	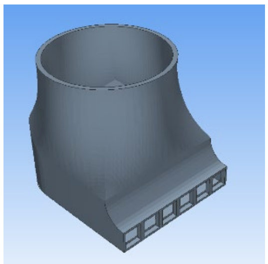

Figure 2: Different designs of under-door exhaust duct.

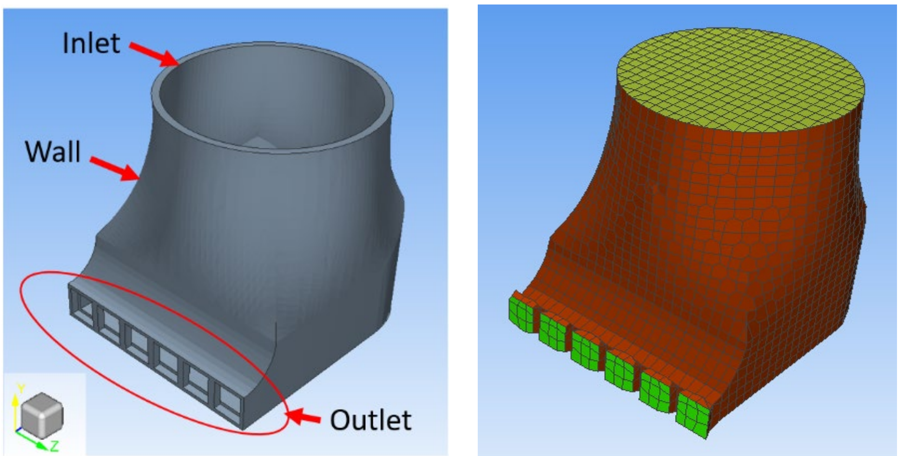

(a) (b)

Figure 3: (a) Boundary conditions and (b) meshed model of the under-door exhaust duct.

Table 1: Meshing data of different models.

Inlet Diameter (mm)	Number hole outlet	Number of nodes	Number of cells	skewness	Aspect ratio
240	2	9294	8276	1.943668	17.10994
	4	9334	8294	1.943668	17.10994
	6	9375	8312	1.943668	17.10994
260	2	9991	8912	1.430506	14.03798
	4	10031	8930	1.430506	14.03798
	6	10072	8948	1.430506	14.03798
280	2	10617	9510	1.126854	13.58962
	4	10657	9528	1.126934	13.58962
	6	10692	9546	1.126854	13.58962

3. RESULTS AND DISCUSSION

The analysis of duct flow using Computational Fluid Dynamics (CFD) reveals several critical insights based on the data provided. Table 2 summarizes the variations in maximum velocity and pressure for different inlet diameters and numbers of outlet holes. The observations are supported by contour plots and graphs, which provide a comprehensive understanding of the flow dynamics within the duct. The data indicates that as the number of outlet holes decreases, both the maximum velocity and pressure increase significantly. For an inlet diameter of 280 mm, the maximum velocity increases from 3.5 m/s with six outlets to 11.1 m/s with two outlets. Similarly, the pressure rises from 7.7 Pa to 85.561 Pa. This trend is consistent across all inlet diameters (280 mm, 260 mm, and 240 mm), demonstrating a clear inverse relationship between the number of outlets and both velocity and pressure.

Figure 4 demonstrates that as the inlet diameter increases from 230 mm to 290 mm, the maximum velocity inside the duct also increases linearly. The equations derived from the data indicate that the velocity increases more significantly with the configuration of two holes compared to four and six holes. Explicitly, the linear relationship for two holes shows an increase in velocity, suggesting that the presence of more holes may lead to a more significant pressure drop, which in turn affects the velocity. Figure 5 reveals a similar linear trend for pressure as the inlet diameter increases. The equations for pressure also indicate a strong correlation, particularly for the 2-hole configuration followed by four holes and six holes. This consistent increase in pressure with larger diameters suggests that a larger inlet allows a greater volume of air to enter the duct, resulting in higher pressure levels.

Figures 6 and 7 focus on the impact of the number of outlet holes on velocity and pressure. Figure 6 illustrates that as the number of outlet holes increases, the maximum velocity inside the duct decreases. The power law equations indicate a strong inverse relationship, particularly for the 240 mm inlet diameter. This trend continues with 260 mm and 280 mm, suggesting that more outlets distribute the airflow more evenly, reducing the velocity. Figure 7 shows that the maximum pressure decreases with increasing outlet holes, following a similar power law relationship. The 240 mm, 260 mm, and 280 mm equations further confirm this trend. The consistent R^2 values indicate a very strong fit, highlighting that as the number of outlets increases, the pressure drops significantly, likely due to the increased area for airflow exit, which reduces resistance and allows for more rapid dissipation of pressure.

In summary, the findings from these graphs emphasize the critical roles that inlet diameter and outlet configuration play in dictating fluid dynamics within duct systems, with larger diameters enhancing both velocity and pressure, while increased outlets lead to reductions in these parameters. To optimize duct design effectively, the Analytical Hierarchy Process (AHP) [14, 15] can be employed to systematically evaluate and prioritize these factors. AHP allows for a structured comparison of various design alternatives, helping to weigh the impact of different inlet diameters and outlet configurations on airflow and pressure management. By integrating AHP into the design process, engineers can make more informed decisions to ensure efficient and effective duct system performance across various applications.

Table 2: Maximum velocity and pressure of different models.

Inlet Diameter (mm)	Number hole outlet	Max velocity (m/s)	Pressure (Pa)
240	2	7.9688	43.9900
	4	4.0094	9.4664
	6	2.5651	3.8664
260	2	9.4752	62.2310
	4	4.7738	13.4120
	6	2.5471	5.4687
280	2	11.1000	85.5610
	4	5.3577	18.5130
	6	3.5000	7.7000

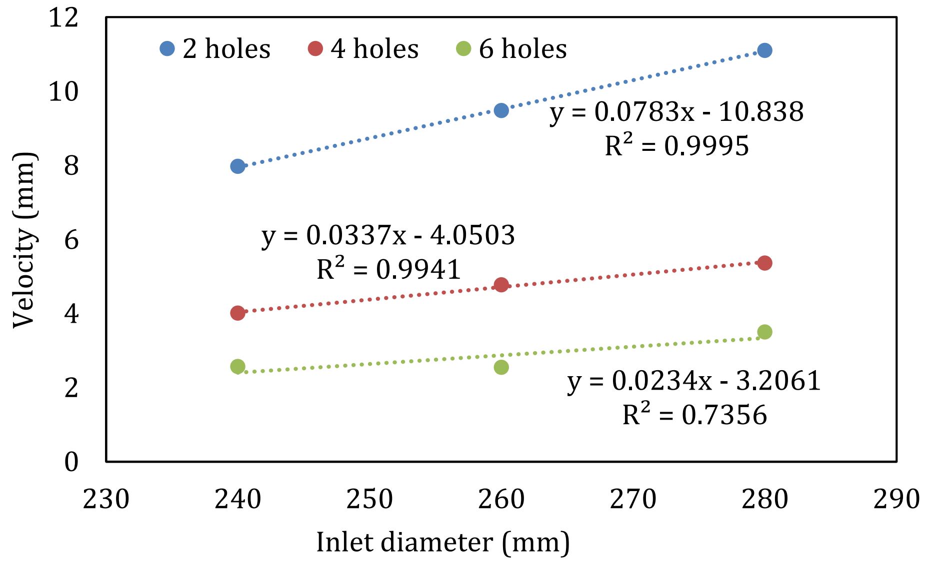

Figure 4: Effect of inlet diameter on the maximum velocity inside the duct.

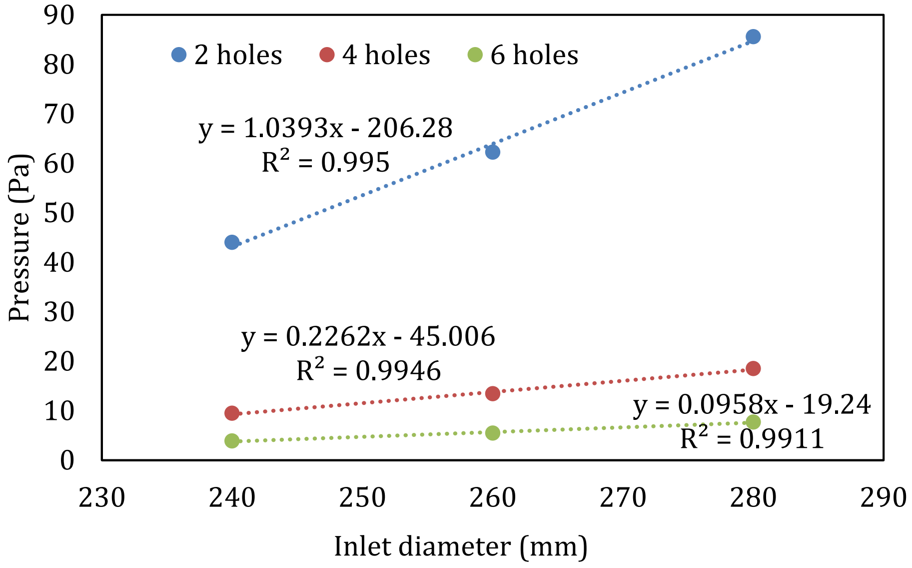

Figure 5: Effect of inlet diameter on the maximum pressure inside the duct.

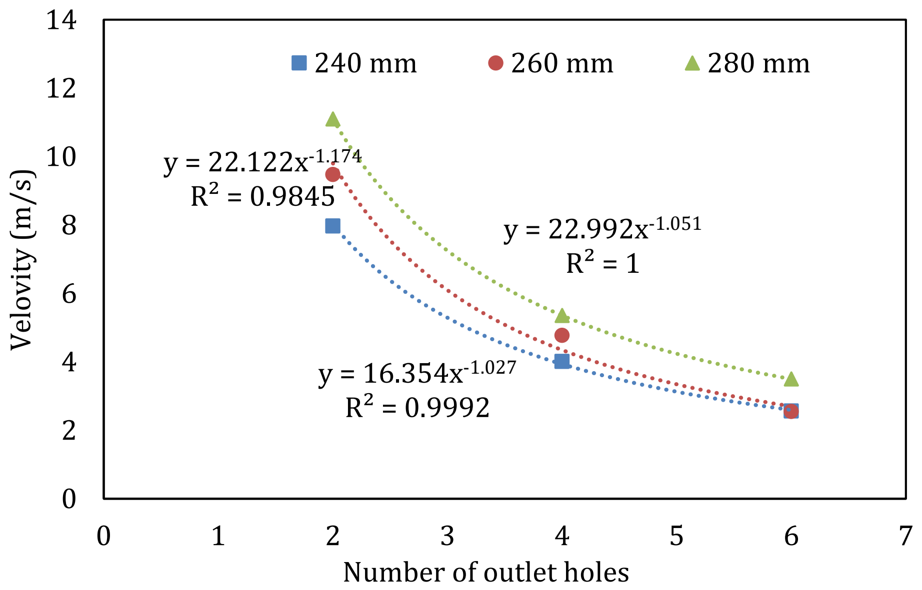

Figure 6: Effect of the number of outlets on the maximum velocity inside the duct.

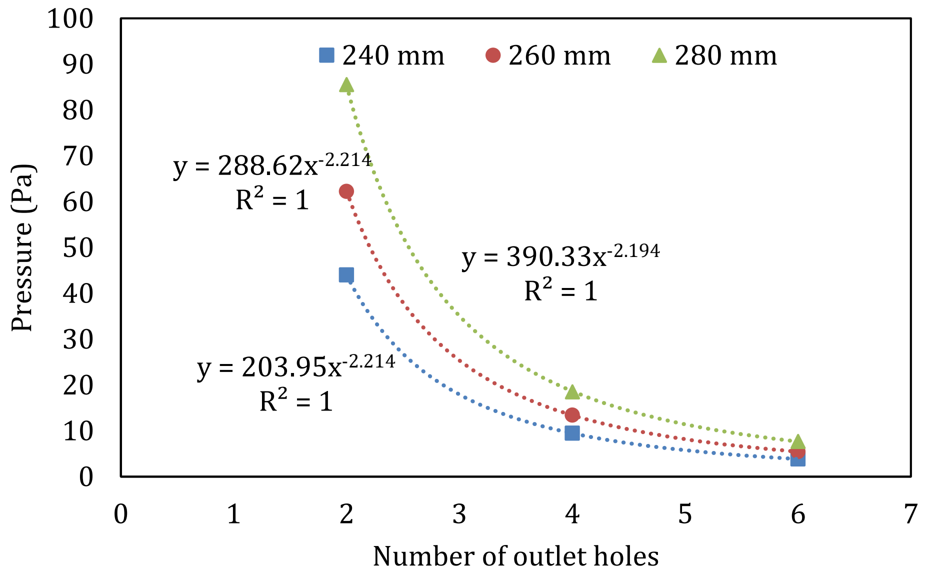

Figure 7: Effect of the number of outlets on the maximum pressure inside the duct.

Figures 8 and 9 illustrate the effects of inlet diameter and the number of outlet holes through velocity and pressure contour. The velocity contour reveals the airflow distribution changes with varying inlet diameters and outlet configurations. Larger inlet diameters show a more uniform velocity distribution across the duct, while configurations with more outlets demonstrate a broader spread of lower velocities, indicating that the airflow is being dispersed more evenly. However, the pressure contour highlights similar trends, with higher pressure zones concentrated near the inlet for larger diameters and lower pressure zones becoming more noticeable with increased outlets. These visual representations reinforce the quantitative findings, illustrating how both inlet diameter and outlet configuration significantly influence the flow characteristics within the duct. The analysis emphasizes the critical roles of inlet diameter and outlet number in determining duct systems' velocity and pressure profiles. Larger inlet diameters enhance both velocity and pressure. At the same time, an increased number of outlets leads to lower velocity and pressure, which is visually supported by the contour maps. This understanding is essential for optimizing duct design for various applications, ensuring efficient airflow management.

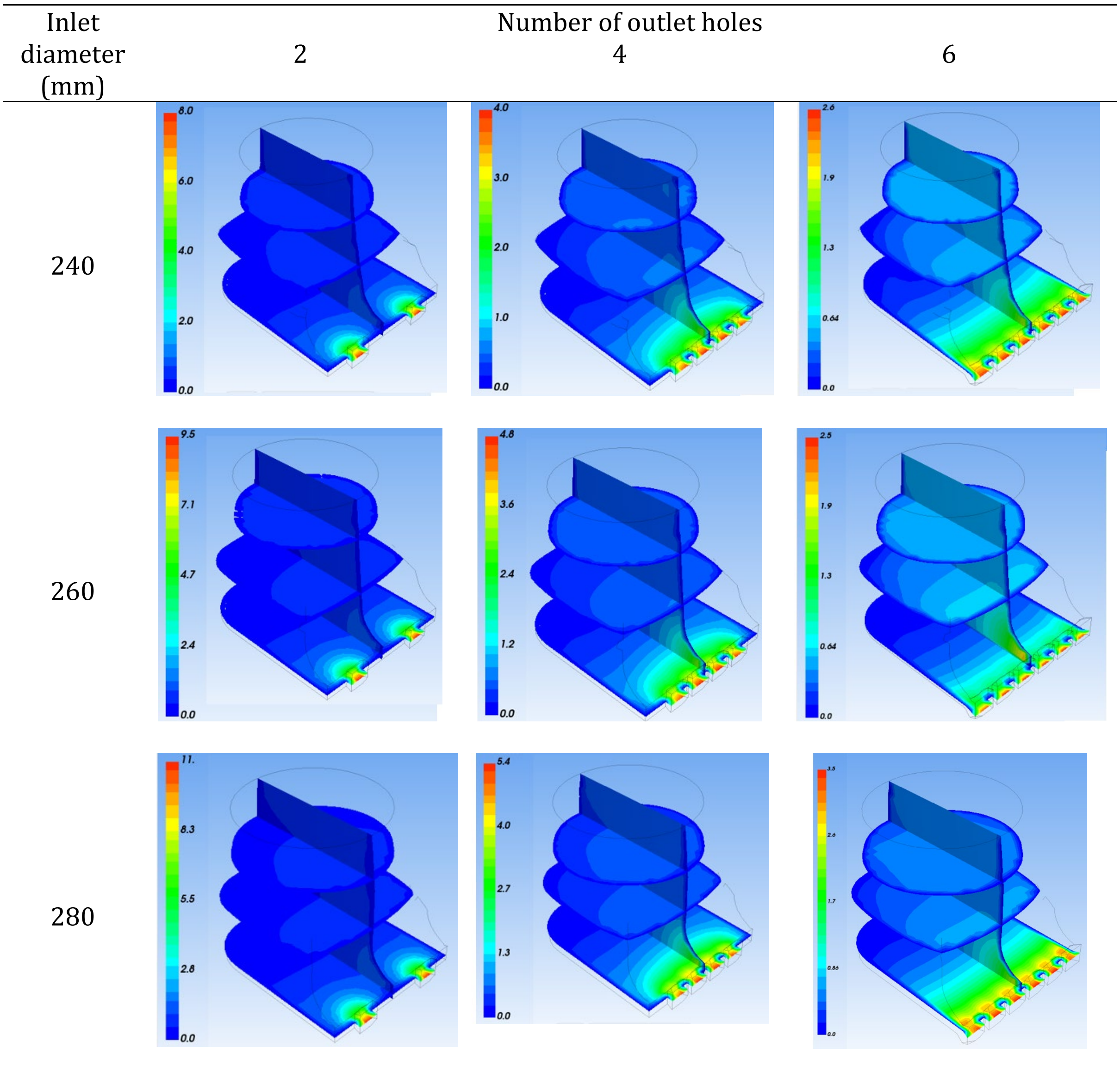

Figure 8: Velocity contour of the duct flow.

Inlet diameter (mm)	Number of outlet holes 2	4	6
240	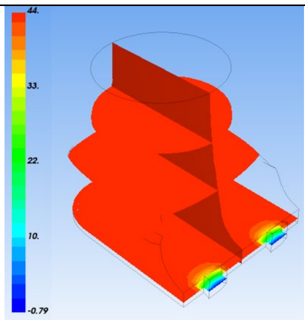	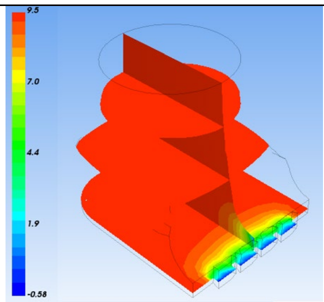	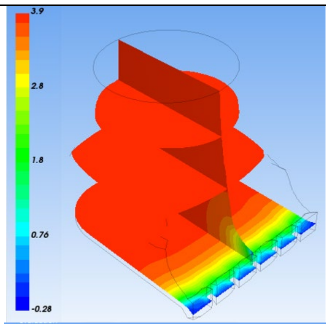
260	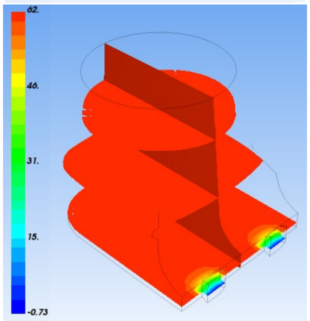	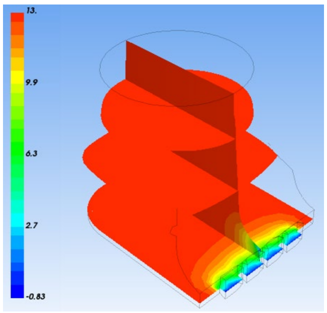	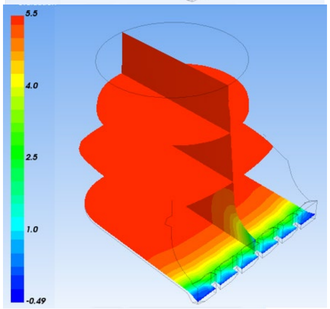
280	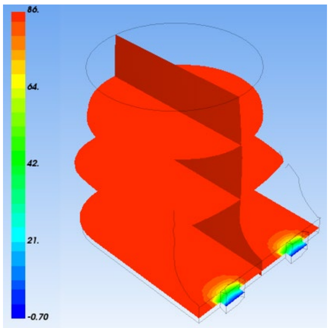	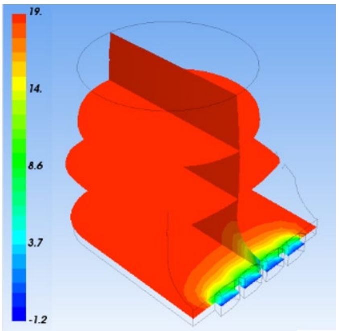	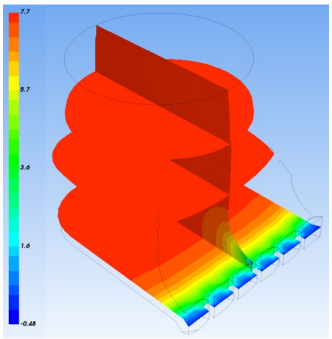

Figure 9: Pressure contour of the duct flow.

4. CONCLUSION

The primary aim of this study was to analyze the effect of the inlet diameter and the number of outlet holes on the velocity and pressure of duct flow using Computational Fluid Dynamics (CFD). By adjusting the inlet diameters (280 mm, 260 mm, and 240 mm) and the number of outlet holes (6, 4, and 2), we observed significant changes in the maximum velocity and pressure within the duct. Our findings showed a clear inverse relationship between the number of outlet holes and both the velocity and pressure. With an inlet diameter of 280 mm, the maximum velocity increased from 3.5 m/s to 11.1 m/s, and the pressure rose from 7.7 Pa to 85.561 Pa as the number of outlets decreased from six to two. Similar trends were observed for the 260 mm and 240 mm inlet diameters, emphasizing the consistent impact of outlet configuration on flow characteristics. Qualitatively, the study demonstrated that fewer outlet holes increase flow resistance, resulting in higher pressure and velocity within the duct. These findings highlight the sensitivity of duct flow to outlet configuration, providing valuable insights for optimizing duct design. The practical implications are significant for engineering applications, particularly in HVAC system design, where efficient duct flow is crucial. Understanding the impact of outlet number and inlet diameter can help engineers design more effective and efficient duct systems, potentially leading to energy savings and improved system performance. For future work, exploring a broader range of inlet diameters and outlet configurations, including non-uniform and variable-diameter ducts, would be beneficial. Besides, investigating the effects of different fluid properties and flow conditions, such as turbulence and temperature variations, could provide a more comprehensive understanding of duct flow dynamics. These extensions would enhance the practical applicability of the findings and contribute to developing more advanced duct system designs.

ACKNOWLEDGEMENTS

The author extends heartfelt gratitude to the Faculty of Mechanical Engineering & Technology for their invaluable support and resources throughout this research. A special thanks to the coordinator of the CFD course, Ts. Dr. Khor Chu Yee for his guidance and mentorship.

REFERENCES

[1] Brankovic, A., STOWERS, S., & McConnaughey, P. SSME 3-D Turnaround Duct flow analysis-CFD predictions. In 24th Joint Propulsion Conference. (1988) p. 3006.
[2] Anand, R. B., Chandraprabhu, A., Richards, X. J. A., & Hareshram, N. Flow and performance characteristics of a Y-shaped diffusing duct using CFD. International Journal of Aerodynamics, vol 1, issue 2 (2010) pp. 115-129.
[3] Gu, T., Chew, Y., Paterson, W., & Wilson, D. Experimental and CFD studies of fluid dynamic gauging in duct flows. Chemical Engineering Science. vol 64, (2009) pp. 219-227.
[4] Avvari, R., & Jayanti, S. Flow apportionment algorithm for optimization of power plant ducting. Applied Thermal Engineering, vol 94, (2016) pp. 715-726.
[5] Devakumaran, P., Balakrishnan, C., Chandran, S., Azhagurajan, C., Veluchamy, B., & Vivekanandan, M. Attainment of fully developed flow in air distribution duct of boiler using CFD analysis. IJARIIE-ISSN (O)-2395-4396, vol 4, issue 2 (2018) pp. 1021-1025.
[6] Boonloi, A., & Jedsadaratanachai, W. Effects of baffle height and baffle location on heat transfer and flow profiles in a baffled duct: a CFD analysis. Modelling and Simulation in Engineering, vol 2022, issue 1 (2022) p. 3698887.
[7] Lopez, N. S., Galeos, S. K., Calderon, B. R., Dominguez, D. R., Uy, B. J., & Iyengar, R. Computational fluid dynamics simulation of indoor air quality and thermal stratification of an underfloor air distribution system (UFAD) with various vent layouts. In Fluid Dynamics & Material Processing, Tech Science Press, vol 17, issue 2 (2021) pp. 333-346.
[8] He, Y., Chu, Y., Zang, H., Zhao, J., & Song, Y. Experimental and CFD study of ventilation performance enhanced by roof window and mechanical ventilation system with different design strategies. Building and Environment, vol 224, (2022) p.109566.
[9] Fan, X., Yu, T., Liu, P., & Li, X. Uniformity of supply air in the plenum for under-floor air distribution ventilation in a circular conference room: a CFD study. Energies, vol 15, issue 17 (2022) p. 6370.
[10] Chau, O. K., Liu, C. H., & Leung, M. K. CFD analysis of the performance of a local exhaust ventilation system in a hospital ward. Indoor and Built Environment, vol 15, issue 3 (2006) 257-271.
[11] Tang, Y. P. Effects of Race Car's Speed on the Aerodynamic Aspect Using Computational Fluid Dynamics Analysis. Advanced and Sustainable Technologies (ASET), vol 3, issue 1 (2024) 54-61.
[12] Tawackolian, K., & Kriegel, M. Turbulence model performance for ventilation components pressure losses. In Building Simulation. Beijing: Tsinghua University Press. vol 15, issue 3 (2022) pp. 389-399.
[13] Sharizal Abdul Aziz, M., Zulkifly Abdullah, M., & Yee Khor, C. Influence of PTH offset angle in wave soldering with thermal-coupling method. Soldering & Surface Mount Technology, vol 26, issue 3 (2014) pp. 97-109.

[14] Rosli, M. U., Jamalludin, M. R., Khor, C. Y., Ishak, M. I., Jahidi, H., Wasir, N. Y., ... & Ismail, R. I. Analytical hierarchy process for natural fiber composites automotive armrest thermoset matrix selection. In MATEC web of conferences. EDP Sciences, vol 97, (2017) p. 01039.

[15] Luqman, M., Rosli, M. U., Khor, C. Y., Zambree, S., & Jahidi, H. Manufacturing process selection of composite bicycle's crank arm using analytical hierarchy process (AHP). In IOP conference series: materials science and engineering, IOP Publishing, vol 318, issue 1 (2018) p. 012058.

Conflict of interest statement: The author declares no conflict of interest.

Author contributions statement: Conceptualization; Methodology; Software; Formal Analysis; Investigation; Writing & Editing, J.Y. Phong.